

Authors are encouraged to submit new papers to INFORMS journals by means of a style file template, which includes the journal title. However, use of a template does not certify that the paper has been accepted for publication in the named journal. INFORMS journal templates are for the exclusive purpose of submitting to an INFORMS journal and should not be used to distribute the papers in print or online or to submit the papers to another publication.

Convex Relaxations for Gas Expansion Planning

Conrado Borraz-Sánchez, Russell Bent, Scott Backhaus
DSA-4: Energy & Infrastructure Analysis, LANL, Los Alamos, NM-87545, USA

Hassan Hijazi, Pascal Van Hentenryck
NICTA and ANU, Canberra, 260, Australia.

Expansion of natural gas networks is a critical process involving substantial capital expenditures with complex decision-support requirements. Given the non-convex nature of gas transmission constraints, global optimality and infeasibility guarantees can only be offered by global optimisation approaches. Unfortunately, state-of-the-art global optimisation solvers are unable to scale up to real-world size instances. In this study, we present a convex mixed-integer second-order cone relaxation for the gas expansion planning problem under steady-state conditions. The underlying model offers tight lower bounds with high computational efficiency. In addition, the optimal solution of the relaxation can often be used to derive high-quality solutions to the original problem, leading to provably tight optimality gaps and, in some cases, global optimal solutions. The convex relaxation is based on a few key ideas, including the introduction of flux direction variables, exact McCormick relaxations, on/off constraints, and integer cuts. Numerical experiments are conducted on the traditional Belgian gas network, as well as other real larger networks. The results demonstrate both the accuracy and computational speed of the relaxation and its ability to produce high-quality solutions.

1. Introduction

In recent years, the construction of natural gas pipelines has witnessed a tremendous growth on a world-wide level. In the U.S., for instance, a \$3 billion expansion project of the gas pipeline system in New England is planned for late 2016. In Europe, the European Investment Bank is supporting a €98 million project for

the expansion of gas pipelines in western Poland, to be completed by 2017. These expansion projects aim at increasing gas flow capacity on existing pipeline systems and/or bringing new gas wells into production and commercialization. In addition, the expansion or reinforcement of a pipeline network can also be considered as a risk-awareness strategy to fulfill short or long-term operational management requirements when unforeseen events occur such as component failures or excessive stress and congestion due to extreme weather conditions. These events were observed in New England during the polar vortex experienced in January 2014, when major gas-fired power plants in the northeast of the U.S. were forced to shut down due to mechanical problems and shortages of gas fuel supplies, which drove wholesale power prices up

According to the U.S. Energy Information Administration (EIA), a project for the development and expansion of a Gas Transmission Network (GTN) takes an average of three years from its first announcement until its completion ([U.S. Energy Information Administration 2008](#)). The project starts by determining the market needs within an open season exercise where nonbinding agreements of capacity rights are offered to potential customers. The second step consists in developing the expansion design with initial financial commitments from the potential customers. Note that expansions of the gas system may include the installation of parallel pipelines along existing ones (also referred to as looping), the addition of compressor stations, the conversion of oil pipelines to natural gas pipelines, or the reinforcement of specific pipeline sections (e.g., replacement of larger diameter pipelines).

In this paper, we address the Gas Transmission Network Expansion Planning (GTNEP) problem where the goal is to fulfill projected future gas contracts and to increase the reliability of a gas system under steady-state conditions. A Mixed-Integer Non-Linear Programming (MINLP) formulation is proposed to model the

design requirements and minimize expansion costs. Given the non-convex nature of the problem, a convex mixed-integer second-order cone relaxation is introduced. The proposed convex relaxation is based on four key ideas: (1) the introduction of variables for modeling the flux directions; (2) exact McCormick relaxations; (3) on/off constraints; and (4) valid integer cuts. Experimental results on the Belgian gas network and a test bed of large-scale synthetic instances demonstrate three key findings:

1. The convex relaxation produces tight lower bounds with high computational efficiency;
2. The solution to the convex relaxation can almost always be used to derive high-quality solutions to the original problem, leading to provably tight optimality gaps and, in some cases, global optimal solutions.
3. The proposed approach scales to large-scale instances.

The rest of this paper is organized as follows. Section 2 presents the literature review. Section 3 introduces the problem formulation. Section 4 specifies the convex relaxation. Section 5 presents the computational results and Section 6 concludes the paper.

2. Literature review

The last four decades have seen an interest in natural gas planning problems such as optimal design, optimal reinforcement, and optimal expansion of gas pipeline systems. Algorithms for these problems can be classified in a number of different ways such as exact approaches (Andre et al. 2009, Bonnans et al. 2011, Edgar et al. 1978, 2001b, Wolf 2004) and heuristics (André 2010, Boyd et al. 1994, Humpola et al. 2015, Andre et al. 2009, Humpola and Fügenschuh 2014a). Exact methods include cutting planes (Atamturk 2002, Humpola and Fügenschuh 2014b, Humpola et al. 2015a, Poss 2011) and branch-and-bound (André 2010, Elshiekh et al. 2013, Humpola and Fügenschuh 2015) and they use a variety of commercial

(Bakhouya and De Wolf 2008, Elshiekh et al. 2013, Soliman and Murtagh 1982) and open-source (Pfetsch et al. 2012, Uster and Dilaveroglu 2014) solvers. Similar to our work, much of the literature relies on approximations and relaxations to improve the tractability of the underlying planning problems. Examples include continuous relaxations of the discrete design variables (De Wolf and Smeers 1996, Hansen et al. 1991, Soliman and Murtagh 1982) and approximation or relaxations of constraints (Babonneau et al. 2012, Bakhouya and De Wolf 2008, Humpola and Fügenschuh 2015, Poss 2011). Common approaches for implementing these approximations/relaxations include successive linear programming (De Wolf et al. 1991, Hansen et al. 1991, O'Neill et al. 1979, Wilson et al. 1988) and piecewise linearizations (Correa-Posada and Sánchez-Martín 2014, Markowitz and Manne 1957, Vajda 1964, Zheng et al. 2010).

The contribution of this paper is a novel Second-Order Cone (SOC) relaxation that efficiently addresses the design of large-scale cyclic networks for which flow directions are unknown. The model captures physical, operational, contractual, and on/off constraints and includes models of regular pipelines, valves, short pipes, control valves, compressor stations, and regulators. Its dual solutions can almost always be converted to high-quality or optimal primal solutions. To the best of our knowledge, the combination of all these features has not appeared in the literature. Our paper focuses on the cost of building the network but can be generalized to include operational costs as well.

We provide next an in-depth review of the most relevant works in the area of natural gas expansion planning problems.

One of the earliest papers that addresses natural gas design problems is (Edgar et al. 1978). This paper focuses on the optimal design of gunbarrel and tree-shaped networks while minimizing the yearly cumulative operational and investment costs. The optimization variables include the number and location of compressor stations,

pipeline diameters, and the inlet and outlet pressures at each compressor station. More recently, Edgar et al. (2001b) solve a simplified version of this problem in GAMS (GAMS Development Corporation 2008) for a small instance (Edgar et al. 2001a).

Hansen et al. (1991) and Soliman and Murtagh (1982) propose a continuous relaxation for the network design problem. While Hansen et al. (1991) apply a successive linear programming method where a linear subproblem is solved to adjust the discrete choice of diameters, Soliman and Murtagh (1982) apply the commercial NLP solver MINOS (Murtagh and Saunders 1998) to handle the relaxed subproblem. O'Neill et al. (1979) and Wilson et al. (1988) focus on a problem where integer variables are used for the operational state of compressor stations and they also implement a method based on successive linear programming to solve the problem.

De Wolf and Smeers (1996) address the optimal dimensioning of a known pipe network topology with an objective that combines the cost of purchasing gas and the capital expenditures for expansion. The authors formulate the problem as a continuous NLP that selects pipeline diameters and solves the problem by means of a local optimizer. Based on this problem, Wolf (2004) derives conditions under which this problem is convex. Through the use of variational inequality theory, the author shows convexity of the nonlinear gas flow system under the assumption that the gas net inlet (pressure) is fixed at all supply and demand nodes. Bakhouya and De Wolf (2008) also present a case study on the same problem with separable transportation and gas objectives that leads to a two-stage problem formulation. In addition to design variables for the optimal pipe diameters, the authors add investment variables representing the maximal power of compressor stations to balance the pipeline construction costs and capital expenditures for increasing power in the compressor units. The authors find an initial solution by solving a convex problem where all pressure constraints are relaxed. Then, the complete problem

is locally solved by means of the GAMS/CONOPT (Drud 1994) solver. In these works, numerical experiments are primarily focused on the Belgian gas transmission network.

Andre et al. (2009) present a MINLP model to solve the investment cost minimization problem for an existing gas system that includes pipelines and regulators and omits compressor stations. The goal is to identify a set of pipeline sections to reinforce and to select an optimal diameter size for these sections based on a discrete set of diameters. Under the assumption that the network is radial (the head loss equations are convex when flows are fixed), the authors propose a continuous relaxation of the pipe diameters (continuous intervals). A branch-and-bound approach for a unique maximal demand scenario is applied to a segment of the French high-pressure natural gas transmission system. A complete review and extensions of these findings are provided in (André 2010).

Babonneau et al. (2009, 2012) focus on the design and operation of a natural gas transmission system while minimizing investment, purchase, and transportation costs. The authors propose an approach based on a minimum energy principle that transforms the non-linear non-convex optimization problem into a convex problem. The underlying convex, bi-objective formulation is an approximation of the investment cost function and the cost of energy to transport the gas. Their continuous formulation is applied to non-divisible constraints such as a limited number of available commercial pipe dimensions.

Bonnans et al. (2011) presents several problems that include the minimization of compressor ratios and the sum of operations and investment costs. The authors propose a global optimization technique that is based on the combination of interval analysis with constraint propagation.

Zheng et al. (2010) discusses different optimization models in the natural gas industry, including the compressor station allocation problem, the least gas pur-

chase problem and optimal dimensioning of gas pipelines. The authors review solution techniques to solve the underlying models which include a piecewise linear programming algorithm and a branch-and-bound algorithm.

Elshiekh et al. (2013) presents a model to optimize the design and operation of the Egyptian gas system, where continuous design variables for the length and diameter of pipelines are considered along with a modified Panhandle equation (Coelho and Pinho 2007). The complete model is directly solved by means of the computer-aided optimization software LINGO (LINDO Systems 1997).

Uster and Dilaveroglu (2014) address the cost minimization problem of designing a new natural gas transmission system and expanding an existing gas system. The authors propose a mathematical formulation to tackle the design/expansion network problem for a given multi-period planning horizon. The underlying MINLP model is formulated in AMPL and solved approximately with Bonmin (Bonami and Lee 2013).

Humpola and Fügenschuh (2014b) and Humpola et al. (2015a) present valid inequalities for a MINLP model of a design problem in gas transmission systems. Different relaxations are applied to the subproblems created after branching on the additive and design variables for the active and passive components. The resulting passive transmission subproblems, which are referred to as leaf problems, admit slack variables to independently relax the pressure domains and the flow conservation constraints. The proposed cutting planes aim at reducing the CPU time of a branch-and-cut-based outer approximation applied to the full model where construction costs are defined by a global constant. Atamturk (2002) and Poss (2011) also propose valid inequalities to reinforce the relaxation approach to the network design structure.

Humpola and Fügenschuh (2015) examines different (convex) relaxations for subproblems created while applying a branch-and-bound technique to a nonlinear

network design problem. Cutting planes on the nonlinear potential loss constraints are used to strengthen the relaxed subproblems.

Pfetsch et al. (2012) focuses on the validation of nomination problem while considering regular pipes and valves, control valves, compressors and regulators. The authors describe a two-stage approach to solve the resulting MINLP problem and propose several modeling techniques and approaches to account for, e.g., pressure losses. They also developed several large test cases (GasLib 2014). These problems form the basis for many of the problems we consider in this paper.

3. Problem Formulation

This section derives the problem formulation in stepwise refinements. It starts by deriving a disjunctive program that is then refined by introducing flux variables.

3.1. Technical bases

Gas dynamics along a pipe is described by a set of partial differential equation (PDE) with both spatial and temporal dimensions (Osładacz 1987, Thorley and Tiley 1987, Sardanashvili 2005):

$$\partial_t \rho + \partial_x(\rho v) = 0, \quad (1)$$

$$\partial_t(\rho v) + \partial_x(\rho v^2) + \partial_x p = -\frac{f}{2D} \rho v |v| - g \sin \alpha \rho, \quad (2)$$

$$p = \mathbf{ZRT} \rho. \quad (3)$$

Gas velocity v , pressure p , and density ρ are defined for every point x along the pipe and evolve over time t . \mathbf{Z} represents the gas compressibility factor, \mathbf{T} the temperature, and \mathbf{R} the gas constant.

Equation (1) enforces mass conservation, Equation (2) describes momentum balance, and Equation (3) defines the ideal gas thermodynamic relation. In Equation (2), the first term on the right-hand side represents the friction losses in a pipe

of diameter D with friction factor f . The second term accounts for the gain or loss of momentum due to gravity g if the pipe is tilted by an angle α . In practice, frictional losses dominate the gravitational term which is dropped. One can also safely assume that the temperature does not fluctuate significantly along a pipe. If temperature gradients are significant, a spatial decomposition, splitting the pipe into temperature stable segments, can be adopted.

Taking into account these assumptions, Equations (1),(2), and (3) are rewritten in terms of pressure p and mass flux $\phi = \rho v$:

$$\partial_t p = -ZRT \partial_x \phi, \quad (4)$$

$$\partial_x p^2 = -\frac{fZRT}{2D} \phi |\phi|, \quad (5)$$

Gas flow equation In this work, we assume that the system has reached a steady state after its first commissioning and hence all time derivatives are set to zero. Given this assumption, a Gas Transmission Network (GTN) is represented by a graph $\mathcal{G} = (\mathcal{N}, \mathcal{A})$ where \mathcal{N} denotes the set of nodes representing connection points and \mathcal{A} denotes the set of arcs. An arc is a triplet (a, i, j) consisting of a unique identifier a linking nodes i and j . For convenience, such a triplet (a, i, j) will be denoted by a_{ij} in the following. Observe that parallel arcs can link the same pair of nodes, e.g., we have arcs a_{ij} and a_{ij}^* in a GTN where a and a^* are the unique identifiers of these arcs.

By setting the time derivatives to zero, the total gas mass flux along a pipe a_{ij} becomes constant, i.e., $\phi_i = \phi_j = \phi_a$. Hence Equations (4) and (5) simplify to

$$p_i^2 - p_j^2 = w_a \phi_a |\phi_a|. \quad (6)$$

where w_a is the flow resistance parameter defined by the physical properties of the pipeline and the volumetric characteristics of the gas and given by (De Wolf and Smeers 2000):

$$w_a = c \left(\frac{D_a^5}{L_a \rho_a} \right),$$

where D_a and L_a correspond to the diameter and length of the pipeline, respectively, $c = \frac{96.074830 \times 10^{-15}}{zTS_g}$ is a constant defined by the compressibility gas factor z , the average gas flowing temperature T and the gas specific gravity S_g , which are all assumed constant in this isothermal flow study. In addition, ρ_a is computed as:

$$\rho_a = 1 \left/ \left[2 \log \left(\frac{3.7D_a}{\epsilon} \right) \right]^2 \right.,$$

with ϵ as the absolute rugosity of the pipeline.

Gas System Components The problem formulation considers *pipes*, *compressors*, *short pipes*, *resistors*, and *valves*. Compressors, short pipes, and valves are modelled as lossless pipelines, i.e., $\mathbf{w}_a = 0$. A compressor installed on arc a_{ij} can increase/decrease the pressure ratio $\alpha_a = p_j/p_i$, within the bounds α_a^l and α_a^u , where $\alpha_a^l = 1$ and $\alpha_a^u \geq 1$ are typical bounds for most compressors. These compressors are modelled as *bi-directional compressors* to perform compression based on the flux direction, i.e., they are able to invert the ratio to $\alpha_a = p_i/p_j$ if the flux is going from j to i .

A standard valve features a binary on/off switch and a *control valve* has a continuous switching mechanism to adjust pressure. Thus a valve installed on arc a_{ij} can increase/decrease the pressure ratio $\alpha_a = p_j/p_i$, within the bounds α_a^l and α_a^u , where $\alpha_a^l > 0$ and $\alpha_a^u \leq 1$ are typical bounds for most control valves and $\alpha_a^l = \alpha_a^u = 1$ for all valves. Finally, a resistor is modelled as a pipeline with a particular (small) loss coefficient (\mathbf{w}).

Expansion Variables The set of arcs $\mathcal{A} = \mathcal{A}_e \cup \mathcal{A}_n$ includes existing arcs $\mathcal{A}_e = \mathcal{P}_e \cup \mathcal{V}_e \cup \mathcal{C}_e$, as well as new arcs $\mathcal{A}_n = \mathcal{P}_n \cup \mathcal{C}_n$. In this notation, \mathcal{P}_e denotes the set of installed pipelines, resistors, and short pipes. \mathcal{V}_e and \mathcal{C}_e denote the set of existing (control and regular) valves and compressors, respectively. \mathcal{P}_n and \mathcal{C}_n denote the set of new pipelines and new compressors, respectively. A binary variable

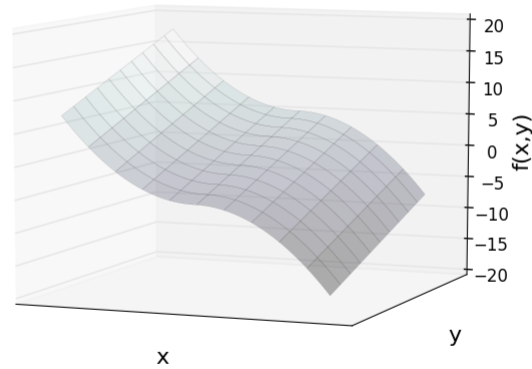


Figure 1 The Gas Flow Equation $f(x, y) = y - wx|x|$.

z_a^p is assigned for each new pipe a_{ij} in \mathcal{P}_n to model the expansion decision, i.e., $z_a^p = 1$ if pipeline a_{ij} is installed and $z_a^p = 0$ otherwise. Variables $z_a^c, \forall a \in \mathcal{C}_n$, have an equivalent interpretation for new compressors. A binary variable v_a is used to control the switching actions of valves.

3.2. The Disjunctive Formulation

We start by observing that the pressure variables only appear in a square form when introducing Equation (6) into the model. Thus, by performing a simple substitution of $\beta_i = p_i^2, \forall i \in \mathcal{N}$, we overcome the non-linearities due to the presence of pressure values. Hence, Equation (6) can be written as

$$\beta_i - \beta_j = \mathbf{w}_a \phi_a |\phi_a| \quad (a_{ij} \in \mathcal{P}_e) \quad (7)$$

Figure 1 illustrates the curve of the function $f(x, y) = y - wx|x|$ defined by the pressure drop equation (7).

Since bi-directional compressor constraints depend on the flux direction, they can only be modelled using on/off or disjunctive constraints (Edgar et al. 2001b, Hijazi et al. 2012). i.e.,

$$\begin{cases} \beta_i \alpha_a^l \leq \beta_j \leq \beta_i \alpha_a^u, & \text{if } \phi_a \geq 0 \\ \beta_j \alpha_a^l \leq \beta_i \leq \beta_j \alpha_a^u, & \text{if } \phi_a \leq 0. \end{cases} \quad (8)$$

Given a set of injection (resp. demand) nodes \mathcal{I} (resp. \mathcal{D}) $\subseteq \mathcal{N}$ with mass flux injection/demand \mathbf{q}_i , the problem consists in finding an assignment of the expansion variables $z_a^p, \forall a_{ij} \in \mathcal{P}_n$, node pressures $p_i, \forall i \in \mathcal{N}$, and edge flows $\phi_a, \forall a_{ij} \in \mathcal{A}$, satisfying the Weymouth equations (7), the compressor constraints (8), and the following node conservation constraints:

$$\sum_{a=a_{ij} \in \mathcal{A}} \phi_a = \sum_{a=a_{ji} \in \mathcal{A}} \phi_a + \mathbf{q}_i, \forall i \in \mathcal{N},$$

where $q_i = 0$ for all $i \in \mathcal{N} \setminus (\mathcal{I} \cup \mathcal{D})$. Note that, in the steady-state flow model, injections are balanced, i.e., $\sum_{i \in \mathcal{N}} \mathbf{q}_i = 0$. The objective is to minimize the cost of expansion:

$$\min \sum_{a \in \mathcal{P}_n} \mathbf{c}_a^p z_a^p + \sum_{a \in \mathcal{C}_n} \mathbf{c}_a^c z_a^c,$$

where \mathbf{c}_a^p and \mathbf{c}_a^c represent the costs of installing a new pipeline and a new compressor, respectively. The disjunctive formulation of the problem incorporating these ideas is presented in Model 1, where $\beta_i^l = (\alpha_i^l)^2$ and $\beta_i^u = (\alpha_i^u)^2$.

Model 1 The Disjunctive Formulation of the GTNEP.

variables:

$\beta_i \in [\beta_i^l, \beta_i^u], \forall i \in \mathcal{N}$ - squared nodal pressure variables

$\phi_a \in \mathbb{R}, \forall a_{ij} \in \mathcal{A}$ - mass flux on pipe (i,j)

$z_a^p \in \{0, 1\}, \forall a \in \mathcal{P}_n$ - binary expansion variables for pipes

$z_a^c \in \{0, 1\}, \forall a \in \mathcal{C}_n$ - binary expansion variables for compressors

$v_a \in \{0, 1\}, \forall a \in \mathcal{CV}_e \cup \mathcal{V}_e$ - binary switch variables for valves

objective:

$$\min \sum_{a \in \mathcal{P}_n} c_a^p z_a^p + \sum_{a \in \mathcal{C}_n} c_a^c z_a^c \quad (9a)$$

subject to:

$$\sum_{a=a_{ij} \in \mathcal{A}} \phi_a = \sum_{a=a_{ji} \in \mathcal{A}} \phi_a + \mathbf{q}_i, \forall i \in \mathcal{N}, \quad (9b)$$

$$\beta_i - \beta_j = \mathbf{w}_a \phi_a |\phi_a|, \forall a_{ij} \in \mathcal{P}_e, \quad (9c)$$

$$z_a^p (\beta_i - \beta_j) = \mathbf{w}_a \phi_a |\phi_a|, \forall a_{ij} \in \mathcal{P}_n, \quad (9d)$$

$$\beta_i \alpha_a^l \leq \beta_j \leq \beta_i \alpha_a^u, \text{ if } \phi_a \geq 0, \forall a_{ij} \in \mathcal{C}_e, \quad (9e)$$

$$\beta_j \alpha_a^l \leq \beta_i \leq \beta_j \alpha_a^u, \text{ if } \phi_a \leq 0, \forall a_{ij} \in \mathcal{C}_e, \quad (9f)$$

$$\beta_i \alpha_a^l \leq \beta_j \leq \beta_i \alpha_a^u, \text{ if } \phi_a \geq 0 \text{ and } z_a^c = 1, \forall a_{ij} \in \mathcal{C}_n, \quad (9g)$$

$$\beta_j \alpha_a^l \leq \beta_i \leq \beta_j \alpha_a^u, \text{ if } \phi_a \leq 0 \text{ and } z_a^c = 1, \forall a_{ij} \in \mathcal{C}_n, \quad (9h)$$

$$\phi_a = 0 \text{ if } z_a^c = 0, \forall a_{ij} \in \mathcal{C}_n, \quad (9i)$$

$$\beta_i \alpha_a^l \leq \beta_j \leq \beta_i \alpha_a^u, \text{ if } \phi_a \geq 0 \text{ and } v_a^c = 1, \forall a_{ij} \in \mathcal{V}_e, \quad (9j)$$

$$\beta_j \alpha_a^l \leq \beta_i \leq \beta_j \alpha_a^u, \text{ if } \phi_a \leq 0 \text{ and } v_a^c = 1, \forall a_{ij} \in \mathcal{V}_e, \quad (9k)$$

$$\phi_a = 0 \text{ if } v_a^c = 0, \forall a_{ij} \in \mathcal{C}_e. \quad (9l)$$

3.3. The Formulation Based on Flux Direction Variables

This section presents a second formulation using flux direction variables to account for the disjunctive nature of the constraints. For every arc $a_{ij} \in \mathcal{A}$, we introduce two binary variables y_a^+ and $y_a^- \in \{0, 1\}$ with the following semantics: $y_a^+ = 1$ (resp. $y_a^- = 1$) if the flux moves from i to j (resp. from j to i) and 0 otherwise. The mass flux direction is captured by the following system of constraints:

$$\left\{ \begin{array}{l} (1 - y_a^+) \sum_{k \in \mathcal{I}} \mathbf{q}_k \leq \phi_a \leq (1 - y_a^-) \sum_{k \in \mathcal{I}} \mathbf{q}_k, \\ (1 - y_a^+) \beta_i^l \leq \beta_i - \beta_j \leq (1 - y_a^-) \beta_i^u, \\ y_a^+ + y_a^- = 1. \end{array} \right.$$

The first constraint ensures that $y_a^+ = 1$ (resp. $y_a^- = 1$) if and only if $\phi_a \geq 0$ (resp. $\phi_a \leq 0$). Note that $\sum_{k \in \mathcal{I}} \mathbf{q}_k$ is an upper bound to the mass flux in a pipe. The second constraint enforces a similar condition for the pressure difference. Using the variables and constraints described above, the pressure drop equation (7) can now be written without absolute value as

$$(y_a^+ - y_a^-) (\beta_i - \beta_j) = \mathbf{w}_a \phi_a^2,$$

and the bi-directional compressor constraints are written as

$$\beta_i \alpha_a^l - (1 - y_a^+) (\beta_i^u \alpha_a^l - \beta_j^l) \leq \beta_j \leq \beta_i \alpha_a^u + (1 - y_a^+) (\beta_j^u - \beta_i^l \alpha_a^u), \forall a_{ij} \in \mathcal{C}_e, \quad (10)$$

$$\beta_j \alpha_a^l - (1 - y_a^-) (\beta_j^u \alpha_a^l - \beta_i^l) \leq \beta_i \leq \beta_j \alpha_a^u + (1 - y_a^-) (\beta_i^u - \beta_j^l \alpha_a^u), \forall a_{ij} \in \mathcal{C}_e, \quad (11)$$

$$\beta_i \alpha_a^l - (2 - y_a^+ - z_a^c) (\beta_i^u \alpha_a^l - \beta_j^l) \leq \beta_j \leq \beta_i \alpha_a^u + (2 - y_a^+ - z_a^c) (\beta_j^u - \beta_i^l \alpha_a^u), \forall a_{ij} \in \mathcal{C}_n, \quad (12)$$

$$\beta_j \alpha_a^l - (2 - y_a^- - z_a^c) (\beta_j^u \alpha_a^l - \beta_i^l) \leq \beta_i \leq \beta_j \alpha_a^u + (2 - y_a^- - z_a^c) (\beta_i^u - \beta_j^l \alpha_a^u), \forall a_{ij} \in \mathcal{C}_n, \quad (13)$$

$$-z_a^c \sum_{k \in \mathcal{I}} \mathbf{q}_k \leq \phi_a \leq z_a^c \sum_{k \in \mathcal{I}} \mathbf{q}_k, \forall a_{ij} \in \mathcal{C}_n. \quad (14)$$

The bi-directional valve constraints are written as

$$\beta_i \alpha_a^l - (2 - y_a^+ - v_a) (\beta_i^u \alpha_a^l - \beta_j^l) \leq \beta_j \leq \beta_i \alpha_a^u + (2 - y_a^+ - v_a) (\beta_j^u - \beta_i^l \alpha_a^u), \forall a_{ij} \in \mathcal{V}_e, \quad (15)$$

$$\beta_j \alpha_a^l - (2 - y_a^- - v_a) (\beta_j^u \alpha_a^l - \beta_i^l) \leq \beta_i \leq \beta_j \alpha_a^u + (2 - y_a^- - v_a) (\beta_i^u - \beta_j^l \alpha_a^u), \forall a_{ij} \in \mathcal{V}_e, \quad (16)$$

$$-v_a \sum_{k \in \mathcal{I}} \mathbf{q}_k \leq \phi_a \leq v_a \sum_{k \in \mathcal{I}} \mathbf{q}_k, \forall a_{ij} \in \mathcal{V}_e. \quad (17)$$

Model 2 The MINLP Formulation of the GTNEP.

variables:

- $\beta_i \in [\beta_i^l, \beta_i^u]$, $\forall i \in \mathcal{N}$ - squared pressure level variables
- $\phi_a \in \mathbb{R}$, $\forall a_{ij} \in \mathcal{A}$ - mass flux on pipe (i,j)
- $z_a^p \in \{0, 1\}$, $\forall a_{ij} \in \mathcal{P}_n$ - binary expansion variables for pipes
- $y_a^+, y_a^- \in \{0, 1\}$, $\forall a_{ij} \in \mathcal{A}$ - binary flux direction variables
- $z_a^c \in \{0, 1\}$, $\forall a_{ij} \in \mathcal{C}_n$ - binary expansion variables for compressors
- $v_a \in \{0, 1\}$, $\forall a_{ij} \in \mathcal{CV}_e \cup \mathcal{V}_e$ - binary switch variables for valves

objective:

$$\min \sum_{a \in \mathcal{P}_n} c_a^p z_a^p + \sum_{a \in \mathcal{C}_n} c_a^c z_a^c \quad (18a)$$

subject to:

$$\sum_{a_{ij} \in \mathcal{A}} \phi_a = \sum_{a_{ji} \in \mathcal{A}} \phi_a + \mathbf{q}_i, \quad \forall i \in \mathcal{N}, \quad (18b)$$

$$(y_a^+ - y_a^-) (\beta_i - \beta_j) = \mathbf{w}_a \phi_a^2, \quad \forall a_{ij} \in \mathcal{P}_e, \quad (18c)$$

$$z_a^p (y_a^+ - y_a^-) (\beta_i - \beta_j) = \mathbf{w}_a \phi_a^2, \quad \forall a_{ij} \in \mathcal{P}_n, \quad (18d)$$

$$(1 - y_a^+) \sum_{k \in \mathcal{I}} \mathbf{q}_k \leq \phi_a \leq (1 - y_a^-) \sum_{k \in \mathcal{I}} \mathbf{q}_k, \quad \forall a_{ij} \in \mathcal{A}, \quad (18e)$$

$$(1 - y_a^+) \beta_i^l \leq \beta_i - \beta_j \leq (1 - y_a^-) \beta_i^u, \quad \forall a_{ij} \in \mathcal{P}, \quad (18f)$$

$$(10) - (17) \quad (18g)$$

$$y_a^+ + y_a^- = 1, \quad \forall a_{ij} \in \mathcal{A}. \quad (18h)$$

The complete Mixed-Integer NonLinear Programming (MINLP) formulation based on flux direction variables is summarized in Model 2. Model 2 is non-convex due to Constraints (18c)-(18d).

4. A Convex Relaxation of the GTNEP

This section introduces a new mixed-integer second-order cone relaxation for Model 2.

4.1. The Variables

For every pipe $a_{ij} \in \mathcal{P}$, the relaxation introduces the auxiliary variable γ_a representing the product in Equations (18c)-(18d), i.e.,

$$\gamma_a = (y_a^+ - y_a^-) (\beta_i - \beta_j), \quad \forall a_{ij} \in \mathcal{P}. \quad (19)$$

This product is then linearized by a standard relaxation introduced by McCormick (1976) for bilinear functions, i.e.,

$$\gamma_a \geq \beta_j - \beta_i + (\beta_i^l - \beta_j^u) (y_a^+ - y_a^- + 1) \quad (20)$$

$$\gamma_a \geq \beta_i - \beta_j + (\beta_i^u - \beta_j^l) (y_a^+ - y_a^- - 1) \quad (21)$$

$$\gamma_a \leq \beta_j - \beta_i + (\beta_i^u - \beta_j^l) (y_a^+ - y_a^- + 1) \quad (22)$$

$$\gamma_a \leq \beta_i - \beta_j + (\beta_i^l - \beta_j^u) (y_a^+ - y_a^- - 1) \quad (23)$$

This linearization is exact, since $(y_a^+ - y_a^-)$ take only discrete values McCormick (1976).

4.2. The Constraints

After substituting γ_a for $(y_a^+ - y_a^-) (\beta_i - \beta_j)$, the non-convex, quadratic, equality constraints (18c) can now be relaxed into

$$\gamma_a \geq \mathbf{w}_a \phi_a^2, \quad \forall a_{ij} \in \mathcal{P}_e. \quad (24)$$

The on/off constraints (18d) represent another challenge for convexifying Model 2. These constraints can be written as

$$\gamma_a = \mathbf{w}_a \phi_a^2 \text{ if } z_a^p = 1, \quad \forall a_{ij} \in \mathcal{P}_n, \quad (25)$$

with a disjunctive second-order cone relaxation defined as

$$\gamma_a \geq \mathbf{w}_a \phi_a^2, \text{ if } z_a^p = 1 \text{ (} a_{ij} \in \mathcal{P}_n \text{)}. \quad (26)$$

Perspective formulations introduced by Hijazi et al. (2012) can be used to formulate the convex hull of such on/off constraints, giving the following rotated second-order cone constraint:

$$z_a^p \gamma_a \geq \mathbf{w}_a \phi_a^2, \forall a_{ij} \in \mathcal{P}_n. \quad (27)$$

The complete Mixed-Integer Second-Order Cone Programming (MISOCP) relaxation is presented in Model 3.

4.3. The Integer Cuts

The MINLP and MISOCP formulations presented in Models 2 and 3 can be strengthened by introducing the following valid integer cuts:

$$\sum_{a_{ij} \in \mathcal{A}} y_a^+ + \sum_{a_{ji} \in \mathcal{A}} y_a^- \geq 1, \forall i \in \mathcal{I} \quad (29)$$

$$\sum_{a_{ji} \in \mathcal{A}} y_a^+ + \sum_{a_{ij} \in \mathcal{A}} y_a^- \geq 1, \forall i \in \mathcal{D} \quad (30)$$

Constraints (29) are generated for each injection node $i \in \mathcal{I}$: They state that at least one connected arc has an outgoing flow, taking the orientation of the arc into account to select the proper variables (y_a^+ for arcs leaving i and y_a^- for arcs coming to i). Constraints (30) follow the same reasoning for demand nodes $i \in \mathcal{D}$.

For a node i with degree two and no injection/demand ($\mathbf{q}_i = 0$), the following integer cut is valid

$$\begin{cases} y_a^+ = y_{a^*}^+ & \text{if } a_{ji}, a_{ik}^* \in \mathcal{A} \\ y_a^+ = y_{a^*}^- & \text{if } a_{ji}, a_{ki}^* \in \mathcal{A} \\ y_a^- = y_{a^*}^+ & \text{if } a_{ij}, a_{ik}^* \in \mathcal{A} \\ y_a^- = y_{a^*}^- & \text{if } a_{ij}, a_{ki}^* \in \mathcal{A} \end{cases} \quad (31)$$

Model 3 The MISOCP Relaxation for the GPNEP.

variables: $\beta_i \in [\beta_i^l, \beta_i^u], \forall i \in \mathcal{N}$ - squared pressure level variables $\phi_a \in \mathbb{R}, \forall a_{ij} \in \mathcal{A}$ - mass flux on pipe (i,j) $z_a^p \in \{0, 1\}, \forall a_{ij} \in \mathcal{P}_n$ - binary expansion variables for pipes $y_a^+, y_a^- \in \{0, 1\}, \forall a_{ij} \in \mathcal{A}$ - binary flux direction variables $\gamma_a \in \mathbb{R}^+, \forall a_{ij} \in \mathcal{P}$ - auxiliary variables for bilinear terms $z_a^c \in \{0, 1\}, \forall a_{ij} \in \mathcal{C}_n$ - binary expansion variables for compressors $v_a \in \{0, 1\}, \forall a_{ij} \in \mathcal{CV}_e \cup \mathcal{V}_e$ - binary switch variables for valves**objective:**

$$\min \sum_{a \in \mathcal{P}_n} c_a^p z_a^p + \sum_{a \in \mathcal{C}_n} c_a^c z_a^c \quad (28a)$$

subject to:

$$(20) - (23), \quad (28b)$$

$$\sum_{a_{ij} \in \mathcal{A}} \phi_a = \sum_{a_{ji} \in \mathcal{A}} \phi_a + \mathbf{q}_i, \forall i \in \mathcal{N}, \quad (28c)$$

$$\gamma_a \geq \mathbf{w}_a \phi_a^2, \forall a_{ij} \in \mathcal{P}_e, \quad (28d)$$

$$z_a^p \gamma_a \geq \mathbf{w}_a \phi_a^2, \forall a_{ij} \in \mathcal{P}_n, \quad (28e)$$

$$-(1 - y_a^+) \sum_{k \in \mathcal{I}} \mathbf{q}_k \leq \phi_a \leq (1 - y_a^-) \sum_{k \in \mathcal{I}} \mathbf{q}_k, \forall a_{ij} \in \mathcal{A}, \quad (28f)$$

$$(1 - y_a^+) \beta_i^l \leq \beta_i - \beta_j \leq (1 - y_a^-) \beta_i^u, \forall a_{ij} \in \mathcal{P}, \quad (28g)$$

$$(10) - (17), \quad (28h)$$

$$y_a^+ + y_a^- = 1, \forall a_{ij} \in \mathcal{A}. \quad (28i)$$

It can be easily derived using the flux conservation constraints (28c) stating that, for a node with degree two and zero injection/demand, the flux direction of the incoming arc determines the flux direction of the outgoing arc.

Finally, we can derive integer cuts for parallel pipelines:

$$y_{a^*}^+ = y_a^+, \quad \forall a_{ij}, a_{ij}^* \in \mathcal{A}. \quad (32)$$

Equations (32) state that parallel pipelines share the same flow direction. The validity of this cut follows from the pressure drop equations (18c) and the fact that parallel pipelines share the same pair of pressure variables.

4.4. Converting the Convex Relaxation into a Feasible Solution to the GTNEP

The solution to the relaxed Model 3 is not always feasible for Model 2. To obtain a feasible solution, we fix all the binary variables and use a nonlinear optimization solver to find a (locally) optimal solution to the resulting problem. In this case, since Model 3 is a relaxation and all variables associated with optimality are fixed, any feasible solution obtained by Model 2 is globally optimal. Note, when the local solver does not converge to a feasible solution, it is possible to use other primal solutions obtained when solving Model 3 and repeat the process to obtain a feasible, locally optimal solution.

5. Computational Experiments

This section studies the performance of the proposed MINLP and MISOCP models and compares them with a model using a piecewise linear approximation. Section 5.1 describes the benchmarks and Section 5.2 the experimental setting and the various algorithms used. Section 5.3 and 5.4 report the computational results on the Belgian network and larger networks respectively, while Section 5.5 reports on the importance of the integer cuts.

5.1. The Benchmarks

5.1.1. The Belgian Network Table 1 shows the list of test instances based on the Belgian network depicted in Figure 2. The table shows, for each benchmark, the number of nodes, sources, terminals, base pipelines, and compressor stations, as well as the number of new components (pipelines and compressors) that can potentially be added to the network topology. Note that benchmark *A* in Table 1 is the real Belgium gas transmission network and Table 3 shows the node characteristics for this 20-node, 24-pipeline, 3-compressor network. The reader is referred to the appendix of (De Wolf and Smeers 2000) for further details on this network. Instances $A_1 - A_3$ captures various possible expansions to this base network. Figure 3 and Tables 5 and 6 depict the location of the potential expansion plans and their associated data. The network expansion plans were designed for the Belgian gas network in order to capture events such as increase of the number of nominations and forecasting demand at the city gates, as well as excessive stress of the available supplies at the sources.

Instances $B_1 - B_4$ are based on the “optimization from scratch” benchmarks from (De Wolf and Smeers 2000) and (Babonneau et al. 2012), where an increasing weighting factor $\alpha = \{1, 1.6, 5, \text{ and } 6\}$, respectively, was used on the investment cost function. In these papers, the authors use the Belgian gas network for a variation of the GTNEP problem that minimizes a combination of operating and expansion costs (the combinations are weighted by α). These benchmarks specify minimum and maximum production levels (see Table 4). Since the GTNEP assumes known gas nomination and production profiles, we computed load and compression profiles based on optimal pressures provided in (Babonneau et al. 2012). Our instances also employ the same cost function as in (Babonneau et al. 2012) to compute the associated costs for building new pipelines, i.e.,

$$L_{ij} (1.04081^{-6} D_{ij}^{2.5} + 11.2155)$$

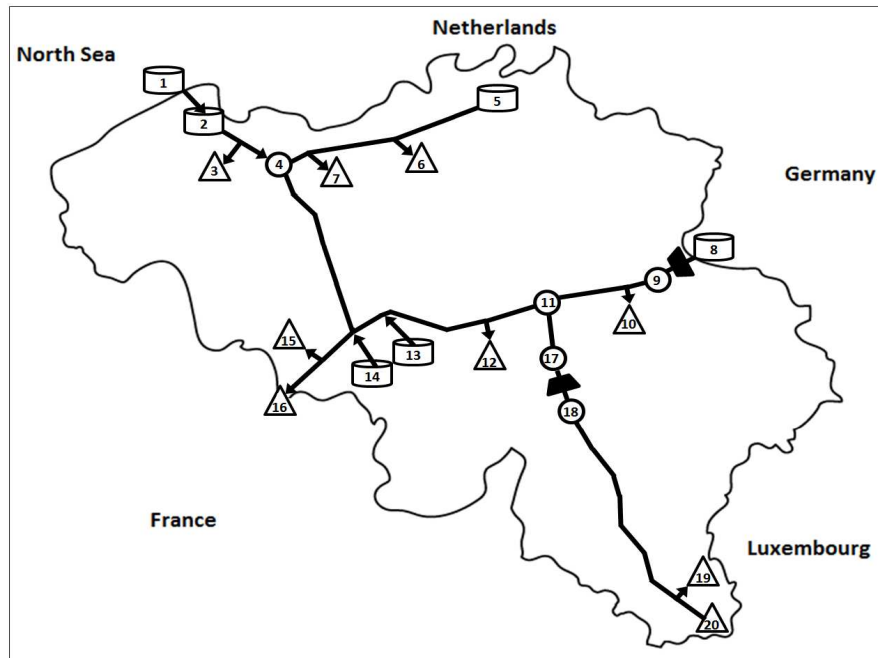


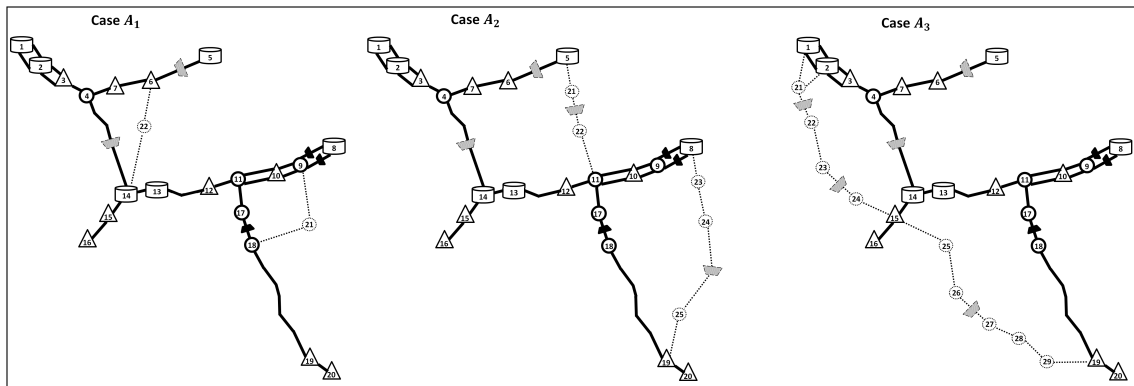
Figure 2 The Belgian Gas Network Base Configuration (case A).

where D_{ij} and L_{ij} are the diameter and length of pipeline (i, j) , respectively. (Babonneau et al. 2012) assumed continuous diameter choices. However, we used discrete diameter values corresponding to the solution of (De Wolf and Smeers 2000) and Table 4 of (Babonneau et al. 2012). For completeness, the diameter choices are described in Table 2. Note that the exclusive-set constraint is slightly different for these cases due to the existence of pre-defined parallel pipes. Within in each row of Table 2, the solution must contain one and only diameter choice, and each set of parallel pipes must choose diameters from the same column of Table 2.

5.1.2. Larger Networks Table 7 describes the main data points for the larger benchmarks. Instance D is a real-life network case whose data is restricted for confidentiality reasons and we are not allowed to disclose its map or load profile. Instances E, F and G are part of a German network whose data, including the

Ref	Network configuration						
	$ \mathcal{N} $	$ \mathcal{I} $	$ \mathcal{D} $	Base		New	
				$ \mathcal{P}_e $	$ \mathcal{C}_e $	$ \mathcal{P}_n $	$ \mathcal{C}_n $
A	20	6	9	24	3	0	0
A_1	22	6	9	24	3	4	2
A_2	25	6	9	24	3	7	4
A_3	29	6	9	24	3	12	5
B_1	20	6	9	0	0	135	12
B_2	20	6	9	0	0	135	12
B_3	20	6	9	0	0	135	12
B_4	20	6	9	0	0	135	12

Table 1 Test Instances Based on the Belgian Network.

Figure 3 The Belgian Gas Network Expansion Plans (Instances A_1 – A_3).

network configuration, maps, and load profiles, can be found in (Pfetsch et al. 2012).

5.2. The Algorithms and the Experimental Setting

This section reports computational results for three approaches:

1. The MINLP formulation of the GTNEP as shown in Model 2;

2. The MISOCP relaxation of the GTNEP as shown in Model 3 followed by the conversion presented in Section 4.4;
3. A MIP formulation based on a Piecewise Linear Approximation (PLA-MIP) of the quadratic functions. The PLA-MIP formulation is based on the PLA-incremental (δ) model derived by Markowitz and Manne (1957), which was shown in (Correa-Posada and Sánchez-Martín 2014) to have computational advantages over its counterpart formulations because of its numerical stability (Keha et al. 2004). We use 60 linear segments based on preliminary computational experiments.

All the experiments were conducted on a computer with two Intel Xeon CPU X5670 processors (2.93GHz) with 6 cores each. The computer has 64 GB DIMM 1333MHz RAM and runs the Ubuntu 14.04 LTS operating system. The MINLP formulation is solved using SCIP 3.1.1 (Achterberg 2009) compiled with Ipopt 3.12.3 and Cplex 12.6. The PLA-MIP formulation is solved using CPLEX 12.6 (ILOG CPLEX Optimization Studio 2013). The MISCOP formulation is solved with CPLEX 12.6 and the conversion is performed by IPOPT 3.12.3 (Wchter and Biegler 2006).

5.3. Results on the Belgian Network

Table 8 shows the sizes of the underlying models in terms of the number of binary and continuous variables and the number of linear and quadratic constraints for each instance. Table 9 presents the computational results and reports the CPU time in seconds and the upgrade cost in $\$ \times 10^3$ for each approach. The computational results show that the MISOCP approach outperforms both the MINLP and the PLA-MIP and that the solution to the MISOCP always converts to a feasible and optimal solution. The PLA-MIP approach has both computational and accuracy issues, as it significantly underestimates the optimal objective value and is rather slow.

The results for problems B1–B4 are interesting as the expansion costs are considerably lower than reported by Babonneau et al. (2012) for the same operating

conditions. In Table 4 of their paper, Babonneau et al. (2012) report expansion costs of 15669, 14252, 11610, and 11274 for B1–B4. Their solutions are feasible and have the same operating cost as our model. Of course, it is important to note that their solutions were obtained through a model that minimizes operating and expansion costs, which could make it harder to determine the best design for particular operating conditions. Still, this comparison highlights the strengths of the formulation proposed in this paper.

5.4. Scalability Results

We now study whether the results on the Belgian networks continue to hold on larger instances. To assess scalability and robustness, we stress the networks by gradually increasing the production and consumption levels from 5% up to 300% while considering solely the addition of a parallel pipe for each existing pipeline in the base configuration of the gas systems (i.e., $|\mathcal{C}_n| = 0$). Table 8 presents the sizes of the mathematical models. In all of these results, we denote whether or not the MISOCP and MINLP solutions are exact, lower bounds, or upper bounds on the MINLP solutions. Lower bounds for the MINLP are also derived by subtracting the optimality gap from any primal feasible solution.

Table 11 presents the computational results on instance D which is based on proprietary natural gas network in the United States. Observe that the PLA-MIP model systematically underestimates the objective function and returns infeasible solutions. As we will see, this is systematic on all larger benchmarks. The MISOCP approach returns optimal solutions for all but one case. Both the MINLP and MISOCP prove infeasibility of the most stressed network.

Table 12 presents the computational results on instance E which is based on gaslib-40 (GasLib 2014). The MISOCP approach returns optimal solutions, or proves infeasibilities in all cases. The MISOCP model is one order of magnitude faster than the MINLP model.

Table 13 presents the computational results on instance F, which is based on gaslib-135 (GasLib 2014) and is particularly challenging. The MINLP approach finds optimal solutions up to the 25% case and spends considerable time doing so. It finds an upper bound to the 50% case but does not return any information on the 75% and 100% cases. In contrast, the MISOCP approach finds optimal solutions to the 0%, 5%, 25%, and 50% cases, all below 10 seconds, It finds lower bounds on the 75% and 100% cases reasonably fast. Both the MINLP and the MISOCP prove infeasibility of the three most stressed instances.

Table 14 presents very interesting results for instance G, which is based on gaslib-582 (GasLib 2014). The MINLP approach cannot find feasible solutions on any of the cases but the 300% case which is shown infeasible. Both the MINLP and PLA-MIP approaches have numerical issues with these problems. The MISOCP approach finds optimal solutions up to the 50% case and for the 150% case and proves infeasibilities for the 200% and 300% cases. For the 75%–125% cases, the MISCOP times out but returns upper bounds to the optimal solution with duality gaps ranging from 7.65% to 51.3%.

Overall, these results demonstrate the benefits of the MISOCP approach. The MISOCP approach almost always finds optimal solutions much faster than the MINLP when both return optimal solutions. It also finds optimal solutions or proves infeasibility in many case for the larger benchmarks, while the MINLP approach does not return feasible solutions.

5.5. The Importance of Integer Cuts

Table 15 describes the performance of the MISCOP on instances E, F, and G when the integer cuts are not used. As can be seen, the integer cuts, which were used both in the MINLP and MISOCP models, are critical to obtain an efficient MISOCP implementation.

6. Concluding Remarks

This paper considered the expansion of natural gas networks, a critical process involving substantial capital expenditures with complex decision-support requirements. It proposed a convex mixed-integer second-order cone relaxation for the gas expansion planning problem under steady-state conditions in order to address the fact that state-of-the-art global optimisation solvers are unable to scale up to real-world size instances. The resulting MISOCP model offers tight lower bounds with high computational efficiency. In addition, the optimal solution of the relaxation can often be used to derive high-quality solutions to the original problem, leading to provably tight optimality gaps and, in some cases, global optimal solutions. The convex relaxation is based on a few key ideas, including the introduction of flux direction variables, exact McCormick relaxations, on/off constraints, and integer cuts. Numerical experiments are conducted on the traditional Belgian gas network, as well as other real larger networks. The computational results demonstrate that the MISOCP model is faster than the originating MINLP model by one or two orders of magnitude on the Belgian network instances. They also show that the MISOCP model scales well to large and stressed instances.

Acknowledgments

This work was in part funded by the Advanced Grid Modeling Program in the Office of Electricity in the US Department of Energy and was in part carried out under the auspices of the National Nuclear Security Administration of the U.S. Department of Energy at Los Alamos National Laboratory under Contract No. DE-AC52-06NA25396.

References

- Achterberg, T. 2009. Scip: Solving constraint integer programs. *Mathematical Programming Computation* **1** 1–41.
- André, J. 2010. Optimization of investments in gas networks. Phd thesis, School in Business, Université Lille Nord de France, France.

- Andre, J., F. Bonnans, L. Cornibert. 2009. Optimization of capacity expansion planning for gas transportation networks. *European Journal of Operational Research* **197** 1019–1027.
- Atamturk, A. 2002. On capacitated network design cut-set polyhedra. *Math. Programming* **92** 425–437.
- Babonneau, F., Y. Nesterov, J.-P. Vial. 2009. Design and operations of gas transmission networks.
- Babonneau, F., Y. Nesterov, J.-P. Vial. 2012. Design and operations of gas transmission networks. *Operations Research* **60** 34–47.
- Bakhouya, B., D. De Wolf. 2008. Optimal dimensioning of pipe networks: the new situation when the distribution and the transportation functions are disconnected. *In: 22th Conference on Quantitative Methods for Decision Making*.
- Bonami, P., J. Lee. 2013. Bonmin – user’s manual.
- Bonnans, J.F., G. Spiers, J.-L. Vie. 2011. Global optimization of pipe networks by the interval analysis approach: The Belgium network case. Tech. rep., Inria Research Report RR-7796, November.
- Boyd, I.D., P.D. Surry, N.J. Radcliffe. 1994. Constrained gas network pipe sizing with genetic algorithms.
- Coelho, P.M., C. Pinho. 2007. Considerations about equations for steady state flow in natural gas pipelines. *J. of the Braz. Soc. of Mech. Sci. & Eng* **XXIX** 262–273.
- Correa-Posada, C.M., P. Sánchez-Martín. 2014. Security-constrained optimal power and natural-gas flow. *IEEE Transactions on Power Systems* **29** 1780–1787.
- De Wolf, D., O. Janssens de Bisthoven, Y. Smeers. 1991. The simplex algorithm extended to piecewise linearly constrained problems i: the method and an implementation. Tech. rep., Universit Catholique de Louvain, Louvain, Belgium.
- De Wolf, D., Y. Smeers. 1996. Optimal dimensioning of pipe networks with application to gas transmission networks. *Operations Research* **44** 596–608.
- De Wolf, D., Y. Smeers. 2000. The gas transmission problem solved by an extension of the simplex algorithm. *Management Science* **46** 1454–1465.
- Drud, A.S. 1994. CONOPT – A large-scale GRG code. *ORSA Journal on Computing* **6** 207–216. doi:10.1287/ijoc.6.2.207.

- Edgar, T.F., D.M. Himmelblau, T.C. Bickel. 1978. Optimal design of gas transmission network. *Society of Petroleum Engineers Journal* 96–104.
- Edgar, T.F., D.M. Himmelblau, L.S. Lasdon. 2001a. <http://www.gams.com/modlib/libhtml/gasnet.htm>.
- Edgar, T.F., D.M. Himmelblau, L.S. Lasdon. 2001b. *Optimization of Chemical Processes. Chapter 9: Mixed-Integer Programming*. 2nd Edition, McGraw-Hill, Boston.
- Elshiekh, T.M., S.A. Khalil, H.A. El Mawgoud. 2013. Optimal design and operation of egyptian gas-transmission pipelines. *Oil and Gas Facilities, Society of Petroleum Engineers* 44–48.
- GAMS Development Corporation. 2008. GAMS: The Solver Manuals.
- GasLib. 2014. Gaslib: A library of gas network instances.
- Hansen, C.T., K. Madsen, H.B. Nielsen. 1991. Optimization of pipe networks. *Mathematical Programming* **52** 45–58.
- Hijazi, H., P. Bonami, G. Cornuéjols, A. Ouorou. 2012. Mixed-integer nonlinear programs featuring on/off constraints. *Computational Optimization and Applications* **52** 537–558. doi:10.1007/s10589-011-9424-0. URL <http://dx.doi.org/10.1007/s10589-011-9424-0>.
- Humpola, J., A. Fügenschuh. 2014a. A new class of valid inequalities for nonlinear network design problems. *Angewandte Mathematik und Optimierung Schriftenreihe (AMOS#4), Applied Mathematics and Optimization Series* .
- Humpola, J., A. Fügenschuh. 2014b. A unified view on relaxations for a nonlinear network flow problem. *Angewandte Mathematik und Optimierung Schriftenreihe (AMOS#6), Applied Mathematics and Optimization Series* .
- Humpola, J., A. Fügenschuh. 2015. Convex reformulations for solving a nonlinear network design problem. *Comput Optim Appl* .
- Humpola, J., A. Fügenschuh, T. Koch. 2015a. Valid inequalities for the topology optimization problem in gas network design. *OR Spectrum* .
- Humpola, J., A. Fügenschuh, T. Lehmann. 2015. A primal heuristic for optimizing the topology of gas networks based on dual information. *EURO J Comput Optim* **3** 53–78.
- ILOG CPLEX Optimization Studio, IBM. 2013. Cplex users manual, version 12 release 6.
- Keha, A.B., I.R. de Farias Jr., G.L. Nemhauser. 2004. Models for representing piecewise linear cost function. *Operations Research Letters* **32** 44–48.

- LINDO Systems. 1997. Lingo 3.1 modeling software.
- Markowitz, H.M., A. Manne. 1957. On the solution of discrete programming problems. *Econometrica* **25** 84–110.
- U.S. Energy Information Administration. 2008. http://www.eia.gov/pub/oil_gas/natural_gas/analysis_publications/ngpipeline/develop.html.
- McCormick, G.P. 1976. Computability of global solutions to factorable nonconvex programs, part i: convex underestimating problems. *Mathematical Programming* **10** 147–175.
- Murtagh, B.A., M.A. Saunders. 1998. Minos 5.5 users guide. Tech. rep., Department of Operations Research, Stanford University, California.
- O’Neill, R.P., M. Williard, B. Wilkins, R. Pike. 1979. A mathematical programming model for allocation of natural gas. *Operations Research* **27** 857–873.
- Osiadacz, A. 1987. *Simulation and analysis of gas networks*. Gulf Pub. Co. URL <http://books.google.com/books?id=cMxTAAAMAAJ>.
- Pfetsch, M.E., A. Fgenschuh, B. Geiler, N. Geiler, R. Gollmer, B. Hiller, J. Humpola, T. Koch, T. Lehmann, A. Martin, A. Morsi, J. Rvekamp, L. Schewe, M. Schmidt, R. Schultz, R. Schwarz, J. Schweiger, C. Stangl, M.C. Steinbach, S. Vigerske, B.M. Willert. 2012. Validation of nominations in gas network optimization: Models, methods, and solutions.
- Poss, M. 2011. Models and algorithms for network design problems. Phd thesis, Faculté des Sciences, Département d’Informatique, Université Libre de Bruxelles, Belgium.
- Sardanashvili, S. A. 2005. *Computational Techniques and Algorithms (Pipeline Gas Transmission) [in Russian]*. FSUE Oil and Gaz, I.M. Gubkin, Russian State University of Oil and Gas.
- Soliman, F.I., B.A. Murtagh. 1982. The solution of large-scale gas pipeline design problems. *Engineering Optimization* **6** 77–83.
- Thorley, A.R.D., C.H. Tiley. 1987. Unsteady and transient flow of compressible fluids in pipelines - A review of theoretical and some experimental studies. *International Journal of Heat and Fluid Flow* **8** 3 – 15. doi:[http://dx.doi.org/10.1016/0142-727X\(87\)90044-0](http://dx.doi.org/10.1016/0142-727X(87)90044-0). URL <http://www.sciencedirect.com/science/article/pii/0142727X87900440>.
- Uster, H., S. Dilaveroglu. 2014. Optimization for design and operation of natural gas transmission networks. *Applied Energy* **133** 56–69.

- Vajda, S. 1964. *Mathematical Programming*. Addison-Wesley.
- Wchter, A., L.T. Biegler. 2006. On the implementation of an interior-point filter line-search algorithm for large-scale nonlinear programming. *Mathematical Programming* **106** 25–57. doi: 10.1007/s10107-004-0559-y. URL <http://dx.doi.org/10.1007/s10107-004-0559-y>.
- Wilson, J.G., J. Wallace, B.P. Furey. 1988. Steady-state optimization of large gas transmission systems. *In: Simulation and optimization of large systems (A.J. Osiadacz Ed)*. Clarendon Press, Oxford.
- Wolf, De. 2004. Mathematical properties of formulations of the gas transmission problem. *SMG Preprint 94/12, Universit Catholique de Louvain, Belgium* .
- Zheng, Q.P., S. Rebennack, N.A. Iliadis, P.M. Pardalos. 2010. Optimization models in the natural gas industry. *In: Handbook of Power Systems I* 121–148.

Pipe	D_1	D_2	D_3	D_4	D_5
(1,2) A	890.0	650.3	610.8	524.7	512.1
(1,2) B	890.0	650.3	610.8	524.7	512.1
(2,3) A	890.0	834.7	784.0	673.5	657.3
(2,3) B	890.0	834.7	784.0	673.5	657.3
(3,4)	890.0	998.9	938.3	806.0	786.7
(5,6)	590.1	604.3	567.6	487.6	475.9
(6,7)	590.1	0	X	X	X
(7,4)	590.1	671.7	630.9	542.0	529.0
(4,14)	890.0	829.9	779.5	669.7	653.6
(8,9) A	890.0	902.8	848.0	728.4	711.0
(8,9) B	395.5	902.8	848.0	728.4	711.0
(9,10) A	890.0	902.8	848.0	728.4	710.9
(9,10) B	395.5	902.8	848.0	728.4	711.0
(10,11) A	890.0	787.6	739.8	635.5	620.1
(10,11) B	395.5	787.6	739.8	635.5	620.4
(11,12)	890.0	979.8	920.3	790.6	771.6
(12,13)	890.0	915.1	859.6	738.4	720.7
(13,14)	890.0	952.6	894.7	768.6	750.1
(14,15)	890.0	1201.0	1128.0	969.0	945.8
(15,16)	890.0	1038.4	975.3	837.9	817.7
(11,17)	395.5	469.0	440.5	378.4	369.3
(17,18)	315.5	469.0	440.5	378.4	369.3
(18,19)	315.5	469.0	440.5	378.4	369.3
(19,20)	315.5	448.9	421.7	362.2	353.5

Table 2 Pipe diameter choices from Table 4 of (Babonneau et al. 2012)

Node (Loc.)	Type ^(*)	(Loads)			(Pressure)	
		\underline{L}	\bar{L}	L	\underline{P}	\bar{P}
1 (Zeebrugge)	\mathcal{I}	8.87	11.594	10.911288	0	77
2 (Dudzele)	\mathcal{I}	0	8.4	8.4	0	77
3 (Brugge)	\mathcal{D}	$-\infty$	-3.918	-3.918	30	80
4 (Zomergem)		0	0	0	0	80
5 (Loenhout)	\mathcal{I}	0	4.8	2.814712	0	77
6 (Antwerp)	\mathcal{D}	$-\infty$	-4.034	-4.034	30	80
7 (Ghent)	\mathcal{D}	$-\infty$	-5.256	-5.256	30	80
8 (Voeren)	\mathcal{I}	20.34	22.01	22.012	50	66.2
9 (Berneau)		0	0	0	0	66.2 [†]
10 (Liège)	\mathcal{D}	$-\infty$	-6.365	-6.365	30	66.2
11 (Warnand)		0	0	0	0	66.2
12 (Namur)	\mathcal{D}	$-\infty$	-2.12	-2.12	0	66.2
13 (Anderlues)	\mathcal{I}	0	1.2	1.2	0	66.2
14 (Péronnes)	\mathcal{I}	0	0.96	0.96	0	66.2
15 (Mons)	\mathcal{D}	$-\infty$	-6.848	-6.848	0	66.2
16 (Blaregnies)	\mathcal{D}	$-\infty$	-15.616	-15.616	50	66.2
17 (Wanze)		0	0	0	0	66.2
18 (Sinsin)		0	0	0	0	63
19 (Arlon)	\mathcal{D}	$-\infty$	-0.222	-0.222	0	66.2
20 (Pétange)	\mathcal{D}	$-\infty$	-1.919	-1.919	25	66.2

Table 3 The Belgian Gas Network Data from (De Wolf and Smeers 2000). This data is used for the A Problems. †- On Problems A1, A2, and A3, the pressure bounds are $[0, 59.851968]$, $[0, 59]$, and $[0, 59.85]$ respectively.

Node	Load (L) profiles (MMscf)			
	B_1	B_2	B_3	B_4
1	9.5883	9.8225	9.8218	9.7205
2	8.1833	8.3447	8.1340	8.3628
3	-3.9180	-3.9180	-3.9180	-3.9180
4	0.0000	0.0000	0.0000	0.0000
5	4.0315	4.0432	4.0383	4.0364
6	-4.0315	-4.0432	-4.0383	-4.0364
7	-5.2413	-5.2644	-5.2562	-5.2644
8	22.012	22.0120	22.0120	22.0120
9	0.0000	0.0000	0.0000	0.0000
10	-6.4744	-6.4951	-6.3970	-6.3816
11	0.0000	0.0000	0.0000	0.0000
12	-2.1929	-2.1191	-2.1162	-2.0984
13	1.2162	1.3225	1.0802	1.1591
14	0.9840	0.6164	1.0776	1.0235
15	-6.4056	-6.5885	-6.8366	-6.8857
16	-15.6119	-15.5904	-15.4616	-15.5899
17	0.0000	0.0000	0.0000	0.0000
18	0.0000	0.0000	0.0000	0.0000
19	-0.2059	-0.2312	-0.2269	-0.2164
20	-1.9337	-1.9112	-1.9131	-1.9236

Table 4 The Load Profiles Computed from Optimal Pressures Provided in (Babonneau et al. 2012).
 All compression ratios were derived as 1.0.

Node	Town	Lat.	Long.	$\underline{P}^{(*)}$	$\overline{P}^{(*)}$
<i>Instance A₁</i>					
21	Bois	50.400676	5.855991	14	66
22	Koninklijke	50.806672	4.481877	14	66
<i>Instance A₂</i>					
21	Heist	51.095651	4.744616	20	70
22	Zoutleeuw	50.858734	5.115404	20	70
23	Beaufays	50.552195	5.670182	20	70
24	Gouvy	50.231757	5.966813	20	70
25	Ettelbruck	49.861370	6.073930	20	70
<i>Instance A₃</i>					
21	Jabbeke	51.204699	3.086440	14	66
22	Torhout	51.072867	3.118026	14	66
23	Kortrijk	50.790711	3.230636	14	66
24	Bois-de-Barry	50.580151	3.521773	14	66
25	Lobbès	50.353208	4.263261	20	70
26	Senzeille	50.124840	4.433550	20	70
27	Gedinne	49.980230	4.851030	20	70
28	Chiny	49.806832	5.274004	20	70
29	Pigneule	49.735878	5.471758	20	70

Table 5 Locations of Nodes of the Expansion Plans for the Belgian Gas Network. These nodes do not have injections.

Node	Node	w	c
<i>Instance A₁</i>			
9	21	0.929	67.19
21	18	0.808	77.26
6	22	0.785	79.50
22	14	0.766	81.44
<i>Instance A₂</i>			
5	21	1.052	59.29
21	21*	Compressor	1500.0
22	11	0.967	64.52
8	23	1.933	32.28
23	24	0.876	71.18
24	24*	Compressor	1500.0
25	19	1.339	46.59
21*	22	0.980	63.65
24*	25	0.866	72.08
<i>Instance A₃</i>			
1	21	2.257	27.65
2	21	4.546	13.73
21	21*	Compressor	1500.0
22	23	1.121	55.66
23	23*	Compressor	1500.0
24	15	1.073	58.14
15	25	1.483	42.09
25	26	1.289	48.40
26	26*	Compressor	1500.0
27	28	1.010	61.79
28	29	2.232	27.96
29	19	1.423	42.09
21*	22	2.448	25.50
23*	24	1.165	53.56
26*	27	1.071	58.28

Table 6 Locations of Pipes of the Expansion Plans for the Belgian Gas Network. * denotes introduced dummy node for 0 length compressor arcs.

Network configuration						
Ref.	Base					New
	$ \mathcal{N} $	$ \mathcal{I} $	$ \mathcal{D} $	$ \mathcal{P}_e $	$ \mathcal{C}_e $	$ \mathcal{P}_n $
<i>D</i>	60	2	24	55	4	55
<i>E</i>	40	3	29	39	6	39
<i>F</i>	135	6	99	141	29	141
<i>G</i>	582	31	129	609	5	278

Table 7 Larger Instances of Gas Networks.

Bench.	MINLP				PLA-MIP				MISOCP			
	BV	CV	LC	QC	BV	CV	LC	QC	BV	CV	LC	QC
<i>A</i>	54	49	254	96	1494	1837	3931	0	54	73	398	24
<i>A</i> ₁	70	59	320	112	1750	2151	4605	0	66	91	488	28
<i>A</i> ₂	85	69	389	124	1945	2391	5120	0	78	107	575	31
<i>A</i> ₃	103	80	463	144	2263	2776	5954	0	91	128	679	36
<i>B</i> _{1,2,3,4}	354	1154	464	357	7314	8737	19067	0	238	373	1850	116

Table 8 The Sizes of the Mathematical models for Belgian Network Instances. (BV: Binary variables, CV: Continuous variables, LC: Linear constraints, QC: Quadratic constraints).

Bench.	MINLP		PLA-MIP		MISOCP	
	CPU	Obj	CPU	Obj	CPU	Obj
<i>A</i>	0.02	0.0	0.6	0.0	0.03	0.0
<i>A</i> ₁	0.06	144	0.7	144	0.05	144
<i>A</i> ₂	0.06	1687	1.4	187	0.1	1687
<i>A</i> ₃	0.06	1780	1.9	280	0.06	1780
<i>B</i> ₁	1.89	11181	1089	10353	0.3	11181
<i>B</i> ₂	3.17	11181	1781	10361	0.6	11181
<i>B</i> ₃	3.53	11181	1538	10352	0.6	11181
<i>B</i> ₄	3.82	11181	1570	10352	0.3	11181

Table 9 Computational Results on the Belgian Network Instances: The Objective Value is in \$ and the CPU Time in Seconds.

Ref.	MINLP				PLA-MIP				MISOCP)			
	BV	CV	LC	QC	BV	CV	LC	QC	BV	CV	LC	QC
<i>D</i>	283	174	1093	440	6883	8330	18018	0	228	339	1753	110
<i>E</i>	207	124	792	312	4887	5920	12796	0	168	241	1260	78
<i>F</i>	763	446	2886	1128	17683	21430	46304	0	622	869	4578	282
<i>G</i>	2101	1469	8058	2256	35941	44433	92848	0	1823	2311	11442	564

Table 10 Size of the Mathematical Models: BV: Binary variables, CV: Continuous variables, LC: Linear constraints, QC: Quadratic constraints.

Stresss level	MINLP		PLA-MIP		MISOCP	
	CPU	Obj	CPU	Obj	CPU	Obj
0%	0.1	0.00★	3.0	0.00	0.1	0.00★
5%	0.5	3.50★	1.8	0.00	0.6	3.50★
10%	1.6	23.83★	12.2	23.22	0.5	23.83★
25%	2.1	92.24★	14.0	83.99	0.6	92.24★
50%	1.5	145.58★	14.8	136.2	0.5	145.58★
75%	0.6	191.80★	11.0	184.0	0.6	191.8★
100%	3.0	287.00★	12.5	209.03	0.7	281.99△
125%	0.2	†	1.6	†	0.2	†

Table 11 Computational Results on Instance D. Obj: $\$ \times 10^6$, CPU time: in seconds, Solution status:

★ = Proven optimal; △ = Lower bound; ▽ = Upper bound; † = Infeasible; ‡ = Unknown.

Stress level	MINLP			PLA-MIP			MISOCP		
	CPU	Obj	Gap	CPU	Obj	Gap	CPU	Obj	Gap
0%	1.6	0.00★	0.0	10.2	0.00	0.0	0.2	0.00★	0.0
5%	6.3	11.92★	0.0	23.5	0.00	0.0	0.7	11.92★	0.0
10%	6.8	32.83★	0.0	20.6	0.00	0.0	0.4	32.83★	0.0
25%	5.6	41.08★	0.0	30.9	32.8	0.0	0.6	41.08★	0.0
50%	8.1	156.06★	0.0	11.5	32.8	0.0	0.9	156.06★	0.0
75%	12.0	333.01★	0.0	21.8	121.1	0.0	0.7	333.00★	0.0
100%	12.1	551.64★	0.0	17.5	122.37	0.0	0.8	551.64★	0.0
125%	2.2	†	–	33.0	256.22	0.0	0.4	†	–
150%	0.8	†	–	27.6	†	–	0.3	†	–

Table 12 Computational Results on Instance E. Obj: $\$ \times 10^6$, CPU time: in seconds, Solution status:

★ = Proven optimal; \triangle = Lower bound; ∇ = Upper bound; \dagger = Infeasible; \ddagger = Unknown.

Stress level	MINLP			PLA-MIP			MISOCP		
	CPU	Obj	Gap	CPU	Obj	Gap	CPU	Obj	Gap
0%	0.85	0.0★	0.0	136.3	0.0	0.0	1.3	0.0★	0.0
5%	101.8	0.0★	0.0	120.0	0.0	0.0	1.0	0.0★	0.0
10%	36707.3	15.04★	0.0	125.8	0.0	0.0	2.4	0.0 \triangle	0.0
25%	457.9	60.4★	0.0	124.4	0.0	0.0	4.4	60.4★	0.0
50%	86962.9	182.7 ∇	91.7	166.7	60.4	0.0	7.6	95.3★	0.0
75%	86933.9	\ddagger	–	119.8	60.4	0.0	40.5	451.5 \triangle	0.0
100%	87334.2	\ddagger	–	119.5	149.6	0.0	104.6	1234.2 \triangle	0.0
125%	6.8	†	–	125.7	149.6	0.0	1.8	†	0.0
150%	3.4	†	–	206.7	486.0	0.0	1.1	†	0.0
200%	0.4	†	–	11.6	†	–	0.4	†	0.0

Table 13 Computational Results on Instance F. Obj: $\$ \times 10^6$, CPU time: in seconds, Solution status:

★ = Proven optimal; \triangle = Lower bound; ∇ = Upper bound; \dagger = Infeasible; \ddagger = Unknown.

Stress level	MINLP			PLA-MIP			MISOCP		
	CPU	Obj	Gap	CPU	Obj	Gap	CPU	Obj	Gap
0%	86400.0	‡	–	62012.9	6.87	0.0	2.7	0.00★	0.0
5%	86400.0	‡	–	29655.1	2.78	0.0	4.4	0.00★	0.0
10%	86400.0	‡	–	86400.0	4.65	40.22	21.1	0.00★	0.0
25%	86400.0	‡	–	2153.2	8.65	0.0	40.9	0.00★	0.0
50%	86400.0	‡	–	3670.2	†	–	164.0	14.93★	0.0
75%	86400.0	‡	–	0.21	†	–	86402.1	111.99▽	51.3
100%	86400.0	‡	–	5.31	†	–	86401.6	332.53▽	7.65
125%	86400.0	‡	–	5.31	†	–	86402.4	524.82▽	11.74
150%	86400.0	‡	–	5.29	†	–	53321.3	590.84★	0.0
200%	86400.0	‡	–	5.02	†	–	16.7	†	–
300%	4.4	†	–	0.12	†	–	0.9	†	–

Table 14 Computational Results on Instance G. Obj: $\$ \times 10^6$, CPU time: in seconds, Solution status: ★ = Proven optimal; Δ = Lower bound; ∇ = Upper bound; \dagger = Infeasible; \ddagger = Unknown.

Stress level	Instance E			Instance F			Instance G		
	CPU	Obj	Gap	CPU	Obj	Gap	CPU	Obj	Gap
0%	0.9	0.00★	0.0	3310.9	0.00★	0.0	242.2	0.00★	0.0
5%	1.8	11.92★	0.0	83.5	0.00★	0.0	14.2	0.00★	0.0
10%	2.7	32.83★	0.0	120.7	0.00 Δ	0.0	301.5	0.00★	0.0
25%	3.2	41.08★	0.0	86419.5	60.44▽	75.1	86400.3	‡	–
50%	8.5	156.06★	0.0	17693.1	95.32★	0.0	8271.05	14.93★	0.0
75%	6.7	333.01★	0.0	86409.9	451.59	59.2	86404.4	111.99▽	79.4
100%	3.8	551.64★	0.0	86404.5	1234.23	44.2	87193.1	332.32▽	87.9
125%	1.8	†	–	90.9	†	–	86401.8	524.82▽	16.1
150%	1.0	†	–	7.5	†	–	86408.9	245.80 Δ	58.5
200%	0.7	†	–	2.0	†	–	13318.6	†	–
300%	0.0	†	–	0.0	†	–	3.0	†	–

Table 15 Computational Results on Instances E, F, and G without the Integer Cuts. Obj: $\$ \times 10^6$, CPU time: in seconds, Solution status: ★ = Proven optimal; Δ = Lower bound; ∇ = Upper bound; \dagger = Infeasible; \ddagger = Unknown